# Protonation of $\eta^5$-Indenyl Ruthenium Hydride Complexes $(\eta^5\text{-}C_9H_7)Ru(L_2)H$ and $\eta^5-\eta^6$ Haptotropic Rearrangement. X-ray Crystal Structures of $(\eta^5\text{-}C_9H_7)Ru(dppm)H$ and $[(\eta^6\text{-}C_9H_8)Ru(dppp)H]^+$

Mei Yuen Hung, Siu Man Ng, Zhongyuan Zhou, and Chak Po Lau*

*Department of Applied Biology & Chemical Technology, The Hong Kong Polytechnic University, Hung Hom, Kowloon, Hong Kong, China*

Guochen Jia*

*Department of Chemistry, The Hong Kong University of Science & Technology, Clear Water Bay, Kowloon, Hong Kong, China*

*Received March 28, 2000*



Protonation of indenyl complexes $(\eta^5\text{-}C_9H_7)Ru(dppm)H$ and $(\eta^5\text{-}C_9H_7)Ru(PPh_3)_2H$ with $CF_3SO_3H$ or $HBF_4{\cdot}Et_2O$ at −60 °C gives the $\eta^2$-dihydrogen complex $[(\eta^5\text{-}C_9H_7)Ru(dppm)(H_2)]^+$ and the dihydride $[(\eta^5\text{-}C_9H_7)Ru(PPh_3)_2H_2]^+$, respectively. Upon warming to room temperature, proton shift from the $\eta^2$-$H_2$ ligand of the former to the indenyl ligand and subsequent migration of the metal fragment from the five-membered ring to the six-membered ring of the indene ligand results in the formation of the $\eta^6$-indene complex $[(\eta^6\text{-}C_9H_8)Ru(dppm)H]^+$. The $PPh_3$ analogue $[(\eta^6\text{-}C_9H_8)Ru(PPh_3)_2H]^+$ is formed in a similar fashion, but in this case, the proton shift is from Ru−H to the indenyl ligand. Low-temperature acidification of $(\eta^5\text{-}C_9H_7)Ru(dppe)H$ and $(\eta^5\text{-}C_9H_7)Ru(dppp)H$ yield mixtures of $\eta^2$-dihydrogen complex and dihydride in both cases. Similar to the dppm and $PPh_3$ analogues, $\eta^6$-indene complexes $[(\eta^6\text{-}C_9H_8)Ru(dppe)H]^+$ and $[(\eta^6\text{-}C_9H_8)Ru(dppp)H]^+$ are generated upon warming solutions of the $\eta^2$-dihydrogen complex/dihydride mixtures to room temperature. In the dppp system, the $\eta^5 \rightarrow \eta^6$ haptotropic rearrangement only occurs after the $\eta^2$-dihydrogen complex → dihydride tautomerization is nearly completed, whereas in the dppe system the two processes seem to occur simultaneously. The parent hydride complexes $(\eta^5\text{-}C_9H_7)Ru(L_2)H$ can be regenerated upon deprotonation of the $\eta^6$-indene complexes with $Et_3N$. Crystal structures of $(\eta^5\text{-}C_9H_7)Ru(dppm)H$ and $[(\eta^6\text{-}C_9H_8)Ru(dppp)H]^+$ have been determined by X-ray crystallography; both complexes have three-legged piano-stool structures.

## Introduction

Protonation of indenyl transition-metal complexes frequently leads to $\eta^5 \rightarrow \eta^6$ haptotropic rearrangement, the result of which is the metal center changing from $\eta^5$-coordination to the five-membered ring of the uninegative indenyl ligand to $\eta^6$-coordination to the six-membered ring of the neutral indene. It has been proposed that the reaction proceeds by initial formation of metal−hydride bond, followed by proton transfer to the indenyl ligand, or by direct proton attack at the indenyl ligand and subsequent migration of the metal fragment from the five-membered ring to the six-membered ring of the indene.[1] We have recently studied the protonation reactions of $(\eta^5\text{-}C_9H_7)Ru(L)_2H$ ($L_2$ = dppm, dppe, dppp, $(PPh_3)_2$). Reported here is the synthesis and characterization of some ruthenium indenyl dihydrogen/dihydride complexes from the protonation reactions and their $\eta^5 \rightarrow \eta^6$ haptotropic rearrangement. Also included are the X-ray structures of the $\eta^5$-indenyl hydride complex $(\eta^5\text{-}C_9H_7)Ru(dppm)H$ and one of the $\eta^6$-indene complexes $[(\eta^6\text{-}C_9H_8)Ru(dppp)H]BF_4$. Although the chemistry of group 8 cyclopentadienyl dihydrogen/dihydride complexes have been extensively studied,[2] that of the analogous indenyl complexes is undoubtedly very underdeveloped.

## Results

**Protonation of $(\eta^5\text{-}C_9H_7)Ru(L_2)H$.** Protonation of $(\eta^5\text{-}C_9H_7)Ru(dppm)H$ (**1**) with $CF_3SO_3H$ in THF-$d_8$ at −60 °C yielded exclusively the dihydrogen complex $[(\eta^5\text{-}C_9H_7)Ru(dppm)(H_2)]CF_3SO_3$ (**5**). The $^1H$ NMR spectrum of **5** at −60 °C showed a broad singlet, which, integrated for two hydrogens at $\delta$ −6.56 ppm, was assignable to $Ru(H_2)$. Variable-temperature $T_1$ measurements on the

(1) (a) Sowa, J. R., Jr.; Angelici, R. J. *J. Am. Chem. Soc.* **1991**, *113*, 2537. (b) Clark, D. T.; Mlekuz, M.; Sayer, B. G.; McCarry, B. E.; McGlinchey, M. J. *Organometallics* **1987**, *6*, 2201. (c) Salzer, A.; Taschler, C. *J. Organomet. Chem.* **1985**. *294*, 261. (d) Yezernitskaya, M. G.; Lokshin, B. V.; Zdanovich, V. I.; Lobanova, I. A.; Kolobova, N. E. *J. Organomet. Chem.* **1985**, *282*, 363. (e) White, C.; Thompson, S. J.; Maitlis, P. M. *J. Chem. Soc., Chem. Commun.* **1976**, 409. (f) Treichel, P. M.; Johnson, J. W. *J. Organomet. Chem.* **1975**, *88*, 207.

(2) (a) Jia, G.; Lau, C. P. *J. Organomet. Chem.* **1998**, *565*, 37. (b) Jia, G.; Lau, C. P. *Coord. Chem. Rev.* **1999**, *190−192*, 83.

10.1021/om000266e CCC: $19.00 
Publication on Web 08/12/2000

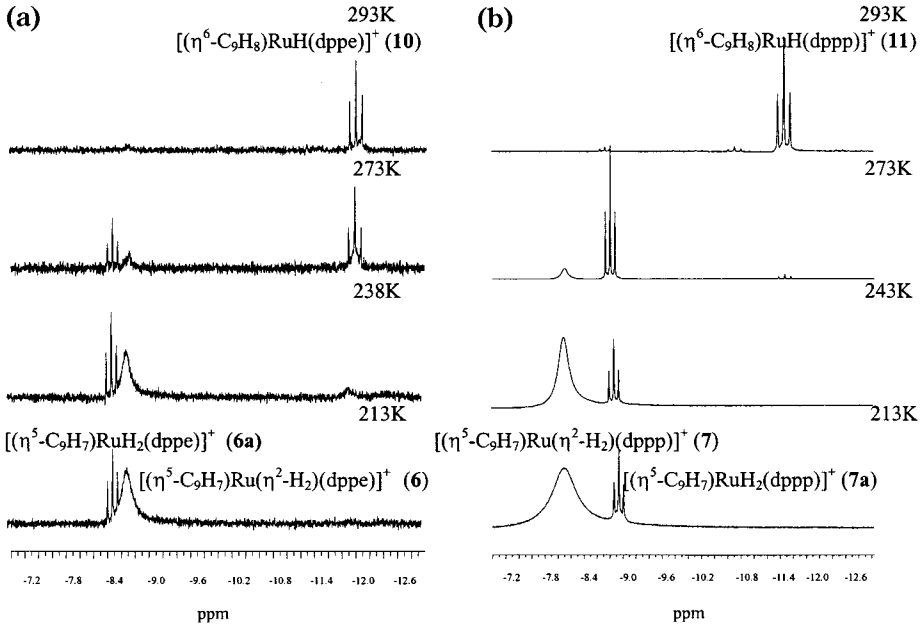


**Figure 1.** Variable-temperature $^1$H NMR spectra of (a) protonation of ($\eta^5$-$C_9H_7$)Ru(dppe)H in THF-$d_8$, (b) protonation of ($\eta^5$-$C_9H_7$)Ru(dppp)H in THF-$d_8$. Only the upfield regions of the spectra are shown.

$\eta^2$-$H_2$ signal gave a minimum $T_1$ value of 13 ms (228 K and 400 MHz). Acidification of **1** with $CF_3SO_3D$ in THF-$d_8$ at −60 °C gave the $\eta^2$-HD isotopomer [($\eta^5$-$C_9H_7$)-Ru(dppm)(HD)]$CF_3SO_3$ (**5-$d_1$**). Its $^1$H NMR spectrum shows a 1:1:1 triplet ($^1J$(HD) = 25.9 Hz) at $\delta$ −6.60 ppm, after nulling the residual $\eta^2$-$H_2$ peak using the inversion−recovery method. The phosphorus atoms of the dppm ligand in **5** appeared as a singlet at $\delta$ 6.7 ppm in the $^{31}$P{$^1$H} NMR spectrum. Based on the $T_1$(min) value, H−H distances of 1.04 and 0.82 Å were estimated for a nonrotating $H_2$ ligand and a freely rotating $H_2$ ligand, respectively.[3] It was estimated to be 0.98 Å using the $^1J$(HD) value.[4]

When the THF-$d_8$ solution of **5** was warmed to room temperature, a new complex, [($\eta^6$-$C_9H_8$)Ru(dppm)H]$CF_3SO_3$ (**9**), with the metal coordinating to the six-membered ring of a neutral indene ligand in a $\eta^6$-bonding mode, was formed at the expense of **5**. The $^1$H NMR spectrum of **9** shows the hydride signal at $\delta$ −9.48 ppm as a triplet of doublets ($^2J$(HP) = 32.3 Hz, $J$(HH) = 3.9 Hz). The hydride is coupled to two equivalent phosphorus atoms and one of the methylene protons of dppm. Coupling of the hydride ligand with one of the methylene protons of dppm has also been observed in Cp*Ru(dppm)H[5] and ($\eta^5$-$C_5H_4(CH_2)_nNMe_2$)Ru(dppm)H ($n$ = 2, 3).[6]

While dppm complex **1** gives the dihydrogen complex **5** on protonation at −60 °C, the dppe and dppp analogues ($\eta^5$-$C_9H_7$)Ru(dppe)H (**2**) and ($\eta^5$-$C_9H_7$)Ru(dppp)H (**3**) yield mixtures of dihydride and dihydrogen complexes, upon acidification with $CF_3SO_3H$ at low temperature (eq 1). The existence of the $\eta^2$-$H_2$ ligand in **6**

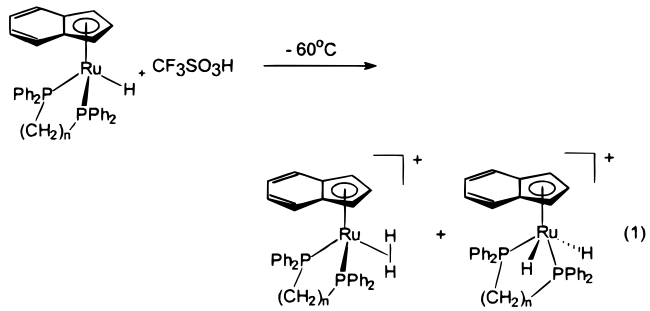


and **7** was confirmed by the small $T_1$(min) values of the their hydride signals in the $^1$H NMR spectra (**6**, $T_1$(min) = 16 ms at 230 K and 400 MHz; **7**, $T_1$(min) = 15 ms at 231 K and 400 MHz) and the large $^1J$(HD) coupling constants for the corresponding HD-isotopomers **6-$d_1$** and **7-$d_1$** (**6-$d_1$**, $^1J$(HD) = 29.4 Hz; **7-$d_1$**, $^1J$(HD) = 27.4 Hz). The hydride complexes **6a** and **7a** show their hydride signals as 1:2:1 triplets at $\delta$ −8.50 ppm ($^2J$(HP) = 29.8 Hz) and $\delta$ −8.90 ppm ($^2J$(HP) = 33.2 Hz), respectively.

The protonation reactions of **2** and **3** were also monitored by variable-temperature $^1$H NMR spectroscopy. It can be seen from Figure 1a that the ratio of the tautomers **6**/**6a** decreases with increasing temperatures. A small broad signal, indicative of a new complex, is clearly visible at around $\delta$ −12 ppm at 238 K. At room temperature, the hydride signals of **6** and **6a** vanish, and the only signal in the hydride region is a triplet at $\delta$ −11.98 ppm, which is assignable to the $\eta^6$-indene complex [($\eta^6$-$C_9H_8$)Ru(dppe)H]$CF_3SO_3$ (**10**). The variable-temperature spectrum in Figure 1b shows that the $\eta^2$-dihydrogen tautomer **7** of the dppp system isomerizes to the dihydride tautomer **7a** with increasing temperature. A new but very small triplet is visible at 273 K. At this temperature most of the dihydrogen complex has isomerized to the dihydride tautomer. However, as the temperature is raised to 293 K, the triplet at $\delta$ −11.37

(3) (a) Hamilton, D. G.; Crabtree, R. H. *J. Am. Chem. Soc.* **1988**, *110*, 4126. (b) Earl, K. A.; Jia, G.; Maltby, P. A.; Morris, R. H. *J. Am. Chem. Soc.* **1991**, *113*, 3027. (c) Desrosiers, P. J.; Cai, L. H.; Lin, Z. R.; Richards, R.; Halpern, J. *J. Am. Chem. Soc.* **1991**, *113*, 4173.

(4) Maltby, P. A.; Schlaf, M.; Steinbeck, M.; Lough, A. J.; Morris, R. H.; Klooster, W. T.; Koetzle, T. F.; Srivastava, R. C. *J. Am. Chem. Soc.* **1996**, *118*, 5396.

(5) (a) Jia, G.; Morris, R. H. *J. Am. Chem. Soc.* **1991**, *113*, 875. (b) Jia, G.; Lough, A. J.; Morris, R. H. *Organometallics* **1992**, *11*, 161.

(6) Chu, H. S.; Lau, C. P.; Wong, K. Y.; Wong, W. T. *Organometallics* **1998**, *17*, 2768.

**Table 1. $^1$H NMR Data ($\delta$, ppm) for Complexes [($\eta^6$-$C_9H_8$)Ru($L_2$)H]$CF_3SO_3$[a]**

| complex | Ru−*H* | *H*$^1$ | *H*$^2$ | *H*$^3$ | *H*$^4$ | *H*$^5$ | *H*$^6$ | *H*$^7$ |
|---|---|---|---|---|---|---|---|---|
| **9**, $L_2$ = dppm | −9.48 (td) (*J*(HP)=32.3 Hz) (*J*(HH)=3.9 Hz) | 6.51 (d) (*J*(HH)=4.9 Hz) | 6.86 (m) | 2.91 (d) (*J*(HH)=23.5 Hz) 3.56 (d) (*J*(HH)=23.5 Hz) | 7.08 (d) (*J*(HH)=3.9 Hz) | 6.46 (m) | 6.46 (m) | 7.05 (d) (*J*(HH)=3.9 Hz) |
| **10**, $L_2$ = dppe | −11.98 (t) (*J*(HP)=35.2 Hz) | 6.06 (d) (*J*(HH)=5.8 Hz) | 6.30 (m) | 2.43 (d) (*J*(HH)=24.0 Hz) 3.75 (d) (*J*(HH)=24.0 Hz) | 6.59 (d) (*J*(HH)=5.9 Hz) | 5.78 (m) | 5.84 (m) | 6.46 (d) (*J*(HH)=5.9 Hz) |
| **11**, $L_2$ = dppp | −11.37 (t) (*J*(HP)=38.2 Hz) | 6.20 (d) (*J*(HH)=5.8 Hz) | 6.25 (m) | 2.22 (d) (*J*(HH)=23.6 Hz) 3.20 (d) (*J*(HH)=23.6 Hz) | 6.61 (d) (*J*(HH)=5.6 Hz) | 5.57 (m) | 5.90 (m) | 6.32 (d) (*J*(HH)=5.6 Hz) |
| **12**, $L_2$ = $(PPh_3)_2$ | −10.25 (t) (*J*(HP)=36.8 Hz) | 5.40 (d) (*J*(HH)=6.0 Hz) | 5.95 (m) | 2.69 (d) (*J*(HH)=23.9 Hz) 3.04 (d) (*J*(HH)=23.9 Hz) | 5.63 (d) (*J*(HH)=6.1 Hz) | 5.77 (m) | 6.00 (m) | 5.44 (d) (*J*(HH)=6.1 Hz) |

[a] Recorded at 400 MHz in THF-$d_8$ at 20 °C; numbering scheme of indene ligand:

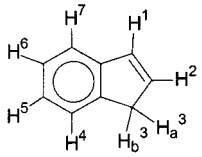




ppm, which is attributable to [($\eta^6$-$C_9H_8$)Ru(dppp)H]$CF_3SO_3$ (**11**), becomes the only signal observed in the hydride region of the $^1$H NMR spectrum. The $^{31}$P{$^1$H} NMR signals of **10** and **11** are singlets at $\delta$ 88.6 and 40.2 ppm, respectively.

In contrast to **1**, the bis(triphenylphosphine) hydride complex ($\eta^5$-$C_9H_7$)Ru$(PPh_3)_2$H (**4**) gave exclusively the dihydride complex *trans*-[($\eta^5$-$C_9H_7$)Ru$(PPh_3)_2(H)_2$]$CF_3SO_3$ (**8**), upon acidification with $CF_3SO_3H$ at −60 °C. The THF-$d_8$ solution of **8** at this temperature gave a high-field triplet ($\delta$ −9.05 ppm, $^2J$(HP) = 26.0 Hz) in the $^1$H NMR spectrum and a singlet at $\delta$ 61.0 ppm in the $^{31}$P{$^1$H} NMR spectrum. On warming to room temperature, the hydride signal of **8** at $\delta$ −9.05 ppm was replaced by a triplet at $\delta$ −10.25 ppm ($^1J$(HP) = 36.8 Hz), while the phosphorus signal at $\delta$ 61.0 ppm in $^{31}$P{$^1$H} NMR spectroscopy yielded a new singlet signal at $\delta$ 57.2 ppm. The new NMR signals can be attributed to the $\eta^6$-indene complex [($\eta^6$-$C_9H_8$)Ru$(PPh_3)_2$H]$CF_3SO_3$ (**12**). Selective $^1$H NMR data for **9**−**12** are collected in Table 1.

It was found that treatment of THF-$d_8$ solutions of [($\eta^6$-$C_9H_8$)Ru($L_2$)H]$CF_3SO_3$ (**9**−**12**) with triethylamine regenerated the $\eta^5$-indenyl complexes **1**−**4** over a period of 1 day, as monitored by $^1$H and $^{31}$P{$^1$H} NMR spectroscopy.

In our attempts to obtain the $\eta^6$-indene complexes in preparative scale, THF solutions of **1**−**4** were acidified with $CF_3SO_3H$ or $HBF_4$·$Et_2O$ at −60 °C, and the resulting solutions were allowed to warm to room temperature. Unfortunately, gummy materials developed upon concentration of the solutions under vacuum, these gummy materials resisted solidification, and attempts to obtain the $\eta^6$-indene complexes in pure form without decomposition were in vain.

**Molecular Structure of 1.** In a preparation of **1**, after collecting the crop by filtration, the mother liquor was allowed to stand, yielding single crystals suitable for an X-ray crystallography study. The X-ray analysis of a crystal of **1** shows two distinct formula units in the unit cell. The bonding in the two units is similar. The molecular structure of one of the formula units is depicted in Figure 2; selected bond distances and angles are given in Table 2. The ruthenium center in **1** is in a distorted pseudooctahedral three-legged piano-stool environment. The hydride ligand was located and refined to give an Ru−H distance of 1.59(2) Å. The two Ru−P bond distances, Ru−P(1) (2.2433(6) Å) and Ru−P(2) (2.2372(6) Å), are slightly shorter than those determined for analogous Cp ruthenium dppm complexes: [CpRu($\eta^2$-dppm)($\eta^1$-dppm)]$PF_6$ (2.295(3), 2.325(3), and 2.323(2) Å),[7] [Cp*Ru(dppm)($\eta^2$-$H_2$)]$BF_4$ (2.314(9) and 2.297(8)

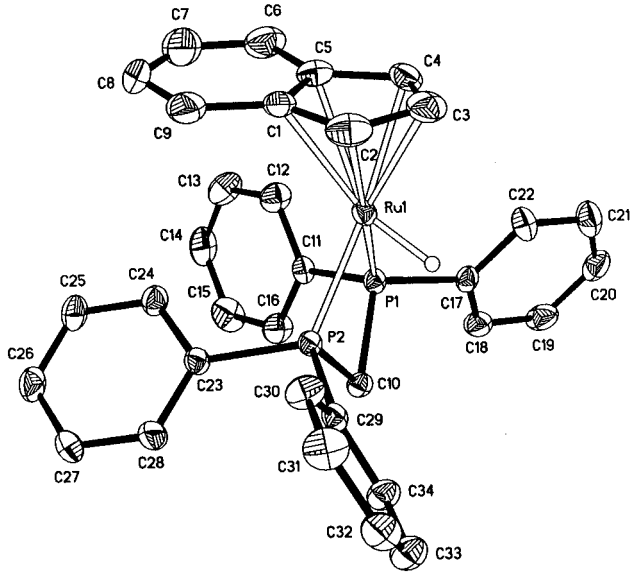


**Figure 2.** Molecular structure of ($\eta^5$-$C_9H_7$)Ru(dppm)H. The thermal ellipsoids are at the 40% probability level.

**Table 2. Selected Bond Distances (Å) and Angles (deg) for Complex 1[a]**

| Bond Distances | | | | | |
|---|---|---|---|---|---|
| Ru−H | 1.59(2) | Ru−C* | 1.9279(2) | Ru−P(1) | 2.2433(6) |
| Ru−P(2) | 2.2372(6) | Ru−C(1) | 2.332(2) | Ru−C(2) | 2.233(2) |
| Ru−C(3) | 2.219(2) | Ru−C(4) | 2.227(2) | Ru−C(5) | 2.326(2) |
| C(1)−C(2) | 1.406(3) | C(1)−C(5) | 1.409(3) | C(2)−C(3) | 1.379(3) |
| C(3)−C(4) | 1.394(3) | C(4)−C(5) | 1.436(2) | C(1)−C(9) | 1.423(3) |
| C(5)−C(6) | 1.379(3) | C(6)−C(7) | 1.352(4) | C(7)−C(8) | 1.396(5) |
| C(8)−C(9) | 1.407(5) | | | | |

| Bond Angles | | | |
|---|---|---|---|
| C*−Ru−P(1) | 144.87(2) | C*−Ru−P(2) | 138.79(2) |
| C*−Ru−H | 119.9 | P(1)−Ru−P(2) | 71.28(2) |
| P(1)−Ru−H | 76.6 | P(2)−Ru−H | 78.8 |
| P(1)−C(10)−P(2) | 89.41(9) | Ru−P(1)−C(10) | 96.65(7) |
| Ru−P(2)−C(10) | 96.78(7) | | |

[a] C* = centroid of C(1), C(2), C(3), C(4), C(5).

Å),[8] and [($\eta^5$:$\eta^1$-$C_5H_4(CH_2)_3NMe_2$)Ru(dppm)]$BPh_4$ (2.3305(8) and 2.3310(8) Å).[6] The P(1)−Ru−P(2) angle of **1** (71.27(2)°) is comparable to those of the Cp analogues: [CpRu($\eta^2$-dppm)($\eta^1$-dppm)]$PF_6$ (70.0(1)°),[7] [Cp*Ru(dppm)($\eta^2$-$H_2$)]$BF_4$ (71.4(3)°),[8] and [($\eta^5$:$\eta^1$-$C_5H_4(CH_2)_3$Ru(dppm)]$BPh_4$ (70.81(3)°).[6] The $\eta^5$-indenyl group coordinates to the metal with only slight slippage toward $\eta^3$-coordination, as shown by the relatively small slip-fold (Δ)[9] value of 0.099 Å, which is similar to those reported for some $\eta^5$-indenyl ruthenium complexes, namely, ($\eta^5$-$C_9H_7$)Ru($PCH_2Ph$)$_3$(CO)I (Δ = 0.07 Å),[10] [($\eta^5$-$C_9H_7$)Ru($PPh_3$)$_2$(CO)]$^+$ [11a] (Δ = 0.10°),[11b] [($\eta^5$-$C_9H_7$)Ru{=C=C−($C_{13}H_{20}$)}($PPh_3$)$_2$]$^+$ (Δ = 0.082 Å),[12] and ($\eta^5$-$C_9H_7$)Ru(C≡CPh)(dppe) (Δ = 0.09 Å).[13] The structure also shows small distortions of the five-carbon ring from planarity with hinge angle (HA)[9] and fold angle (FA)[9] equal to 5.5° and 6.9°, respectively.

**Molecular Structure of [($\eta^6$-$C_9H_8$)Ru(dppp)H]$^+$.** Although our attempts to obtain pure $\eta^6$-indene complexes by protonation of **1**−**4** in preparative scale have not been successful, we have, however, been able to obtain X-ray grade single crystals of the $\eta^6$-indene complex [($\eta^6$-$C_9H_8$)Ru(dppp)H]$BF_4$·$CH_2Cl_2$ from the NMR tube. Thus, after the conclusion of a VT NMR study of the protonation reaction of ($\eta^5$-$C_9H_7$)Ru(dppp)H (**3**) with $HBF_4$·$Et_2O$ in THF-$d_8$, the solvent was removed under vacuum, the residue was redissolved in a minimum amount of $CH_2Cl_2$ in the NMR tube, and crystals suitable for an X-ray diffraction study were obtained by layering of hexane on the solution. Figure 3 shows the molecular structure of the cation [($\eta^6$-$C_9H_8$)Ru(dppp)H]$^+$, and selected bond distances and angles are given in Table 3. Like **1**, the cation exhibits a three-legged piano-stool geometry. The hydride ligand was located and refined to give a Ru−H bond distance of 1.47(2) Å. Both the six-membered and five-membered rings of the indene ligand are essentially planar. Deviations of the carbon atoms from the least-squares plane range from 0.0076 to 0.0090 Å in the former, while deviations of the carbon atoms from the plane fall in the range 0.0029−0.0099 Å in the latter. The two rings are slightly folded along the bridgehead carbon atoms, C(5) and C(9), with an angle of 3.9°. The two hydrogen atoms on C(6) are located but not refined. The C(7)−C(8) bond in the five-membered ring shows the largest double-bond character, as illustrated by the relatively short C−C bond distance of 1.343(4) Å. The six-membered ring does not show obvious alternation in the C−C distances, which lie in the range 1.388(3)−1.407(4) Å. It is bound to the Ru(dppp)H fragment in an unsymmetrical mode, the three carbon atoms C(1), C(5), and C(9) being significantly further (ca. 2.33−2.34 Å) from the Ru than the other three carbon atoms C(2)−C(4) (ca. 2.23−2.26 Å), among which C(2) and C(3) are 2.229(3) and 2.233(3) Å from the metal center, respectively. Unsym-

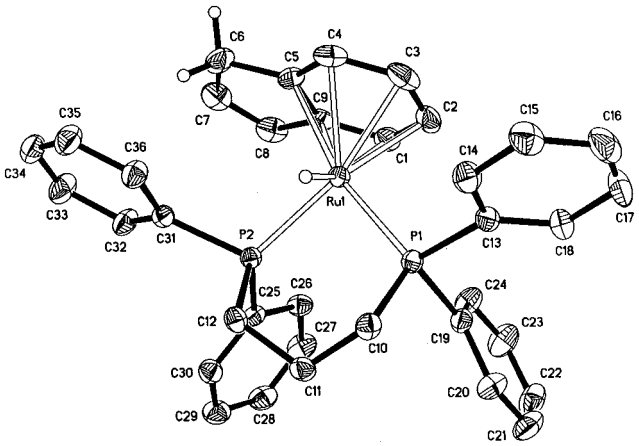


**Figure 3.** Molecular structure of the cation [($\eta^6$-$C_9H_8$)Ru(dppp)H]$^+$. The thermal ellipsoids are at the 40% probability level.

**Table 3. Selected Bond Distances (Å) and Angles (deg) for [($\eta^6$-$C_9H_8$)Ru(dppp)H]$^+$[a]**

| Bond Distances | | | | | |
|---|---|---|---|---|---|
| Ru−C* | 1.8124(2) | Ru−H | 1.47(2) | Ru−P(1) | 2.2779(5) |
| Ru−P(2) | 2.2863(6) | Ru−C(1) | 2.337(2) | Ru−C(2) | 2.233(3) |
| Ru−C(3) | 2.228(3) | Ru−C(4) | 2.261(3) | Ru−C(5) | 2.328(2) |
| Ru−C(9) | 2.335(2) | C(1)−C(2) | 1.393(3) | C(1)−C(9) | 1.388(3) |
| C(2)−C(3) | 1.388(4) | C(3)−C(4) | 1.407(4) | C(4)−C(5) | 1.399(3) |
| C(5)−C(9) | 1.400(3) | C(5)−C(6) | 1.513(3) | C(6)−C(7) | 1.419(4) |
| C(7)−C(8) | 1.344(4) | C(8)−C(9) | 1.479(3) | | |

| Bond Angles | | | |
|---|---|---|---|
| C*−Ru−P | 131.33(2) | C*−Ru−P(2) | 134.65(1) |
| C*−Ru−H | 124.1 | P(1)−Ru−H | 80.3 |
| P(2)−Ru−H | 75.1 | P(1)−Ru−P(2) | 89.28(2) |
| C(5)−C(6)−C(7) | 104.1(2) | C(5)−C(9)−C(8) | 107.88(19) |
| C(6)−C(7)−C(8) | 113.1(2) | C(6)−C(5)−C(9) | 107.35(19) |
| C(7)−C(8)−C(9) | 107.5(2) | | |

[a] C* = centroid of C(1), C(2), C(3), C(4), C(5), C(9).



(7) Bruce, M. I.; Cifuentes, M. P.; Grundy, K. R.; Liddell, M. J.; Snow, M. R.; Tiekink, E. R. T. *Aust. J. Chem.* **1988**, *41*, 597.

(8) (a) Jia, G.; Lough, A. J.; Morris, R. H. *Organometallics* **1992**, *11*, 161. (b) Klooster, W. T.; Koetzle, T. F.; Jia, G.; Fong, T. P.; Morris, R. H.; Albinati, A. *J. Am. Chem. Soc.* **1994**, *116*, 7677.

(9) (a) Δ is *d*[Ru−$C_{av}$(C1, C5)] − *d*[Ru−$C_{av}$(C2, C4)]; HA is the angle between normals to least-squares planes defined by C2, C3, C4 and C1, C2, C4, C5; FA is the angle between normals to least-squares planes defined by C2, C3, C4 and C1, C5, C6, C7, C8, C9. For early work on using Δ, HA, and FA to define slip-fold distortion, see: (b) Faller, J. W.; Crabtree, R. H.; Habib, A. *Organometallics* **1985**, *4*, 929. (c) Baker, R. T.; Tulip, T. H. *Organometallics* **1986**, *5*, 839. (d) Marder, T. B.; Calabrese, J. C.; Roe, D. C.; Tulip, T. H. *Organometallics* **1987**, *6*, 2012. (d) Marder, T. B.; Williams, I. D. *J. Chem. Soc., Chem. Commun.* **1987**, 1478. (e) Kakkar, A. K.; Jones, S. F.; Taylor, N. J.; Collins, S.; Marder, T. B. *J. Chem. Soc., Chem. Commun.* **1989**, 1454. (f) Kakkar, A. K.; Taylor, N. J.; Calabrese, J. C.; Nugent, W. A.; Roe, D. C.; Connaway, E. A.; Marder, T. B. *J. Chem. Soc., Chem. Commun.* **1989**, 990. (g) Westcott, S. A.; Kakkar, A. K.; Stringer, G.; Taylor, N. J.; Marder, T. B. *J. Organomet. Chem.* **1990**, *394*, 777.

(10) Loonat, M. S.; Carlton, L.; Boeyens, J. C. A.; Coville, N. J. *J. Chem. Soc., Dalton Trans.* **1989**, 2407.

(11) (a) Oro, L. A.; Ciriano, M. A.; Campo, M.; Foces-Foces, C.; Cane, F. H. *J. Organomet. Chem.* **1985**, *289*, 117. (b) Δ is calculated from X-ray data of [($\eta^5$-$C_9H_7$)Ru($PPh_3$)$_2$(CO)]$^+$ in ref 11a.

(12) Cadierno, V.; Gamasa, M. R.; Gimeno, L.; Lastra, E.; Borgo, J.; Garcia-Granda, S. *Organometallics* **1994**, *13*, 745.

(13) Tanase, T.; Mochizuki, H.; Sato, R.; Yamamoto, Y. *J. Organomet. Chem.* **1994**, *466*, 233.

metrical coordination of the metal fragment with the six-membered ring of indene or indenyl ligand have also been observed in other complexes, but in these complexes, the bond distances between the metal and the two bridgehead carbon atoms are significantly longer than those between the former and the other four carbon atoms of the ring; that is, the metal shows slippage toward $\eta^4$-coordination to the six-membered ring.[14] The P(1)−Ru−P(2) angle (89.28(2)°), which is much larger than that of **1** (71.27(2)°), is in consonance with the well-known phenomenon that P−M−P angles in three-legged piano-stool complexes with larger chelating diphosphines are much larger than the corresponding angles in similar complexes containing the dppm ligand.

## Discussion

Protonation of indenyl ruthenium complexes of the formula $[(\eta^5\text{-}C_9H_7)Ru(L_2)(H)]$ can, in principle, occur at a variety of sites; oxidative addition of a proton to the metal center generates the dihydride complex, while proton attack at the hydride ligand leads to the formation of the nonclassical dihydrogen complex,[15] and finally if the site of proton attack is the indenyl ligand, the $\eta^6$-indene complex $[(\eta^6\text{-}C_9H_8)Ru(L_2)(H)]^+$ would be formed after the metal fragment migrates from the five-membered ring to the six-membered ring of the indene ligand. This kind of indenyl protonation and subsequent hapotropic migration has been observed in protonation of the $\eta^5$-indenyl manganese complex $(\eta^5\text{-}C_9H_7)Mn(CO)_3$.[1d]

The protonation reactions of related ruthenium cyclopentadienyl hydride complexes $(\eta^5\text{-}C_5R_5)Ru(L)(L')H$ have been extensively studied, but those of the indenyl analogues have been rarely reported. Previous studies have shown that, depending on the nature of the ligands, the compositions of the final protonation products at ambient temperatures may adopt the dihydrogen form $[(\eta^5\text{-}C_5R_5)Ru(L)(L')(H_2)]^+$ or the dihydride form *trans*-$[(\eta^5\text{-}C_5R_5)Ru(L)(L')(H)_2]^+$, or a mixture of both.[2] The initial protonation products may, however, be quite different from the final thermodynamic ones. Chinn and Heinekey have studied the protonation of a series of ruthenium complexes of the types Cp*Ru(L)(L′)H and CpRu(L)(L′)H at 195 K and have found out in every case that the kinetic product is the dihydrogen complex, but an intramolecular isomerization occurs to give variable amounts of the transoid dihydride form in equilibrium. For example, protonation of $Cp'Ru(PPh_3)_2H$ (Cp′ = Cp, Cp*) at 195 K led to exclusive formation of the dihydrogen complexes $[Cp'Ru(PPh_3)_2(H_2)]^+$, and isomerization to the transoid dihydride was observed for $[CpRu(PPh_3)_2(H_2)]^+$ and $[Cp^*Ru(PPh_3)_2(H_2)]^+$ at 222 and 253 K, respectively, and proceeded to completion upon warming to ambient temperature.[16]

In the protonation reactions of indenyl complexes **1**−**4** at −60 °C, the initial products are $\eta^2$-dihydrogen complex, dihydride, or mixtures of both. Products of direct proton attack at the indenyl ligand have never been observed in our studies, although it is also a potential site of proton attachment. However, in warming the solutions to room temperature, the initial products **5**−**8** are converted to the $\eta^6$-indene hydride complexes **9**−**12** via $\eta^5 \rightarrow \eta^6$ haptotropic rearrangement. Such rearrangement is a combination of proton transfer from the metal fragment to an endo position of the indenyl ligand and migration of the former from the five-membered ring of indene to the six-membered one. Migration of the metal fragment from one ring to the other in indene has been studied by extended Hückel methods. It has been shown that the most favored pathway involves migration via the periphery of the rings, not the one across the center of the bond shared by two rings.[17]

The proton transfer from the metal fragment to the indenyl ligand may go through the dihydrogen intermediate or the dihydride intermediate. In the haptotropic rearrangement of $[(\eta^5\text{-}C_9H_7)Ru(dppm)(H_2)]CF_3SO_3$ (**5**), the proton is likely transferred to the indenyl ligand directly from the $\eta^2$-$H_2$ ligand, although transfer from transient dihydride intermediate could not be completely excluded. Proton transfers from the $\eta^2$-$H_2$ ligand to other intramolecular organic ligands have been reported. For instance, transfer of a proton from the $\eta^2$-$H_2$ ligand to the α-carbon of alkyl or vinyl ligands has been invoked to explain the catalytic activity of $[Fe(PP_3)(H_2)H]^+$ ($PP_3 = P(CH_2CH_2PPh_2)_3$[18] and $RuHCl(PPh_3)_3$[19] in hydrogenation of olefins and acetylenes. A $\sigma$-bond metathesis reaction between $\eta^2$-$H_2$ and the metal−alkyl bond has also been proposed for the reactions of some $d^0$ alkyl complexes with $H_2$ to give hydride complexes and alkanes.[20] In the course of $\eta^5 \rightarrow \eta^6$ haptotropic rearrangement, no isomerization of the dihydrogen complex $[(\eta^5\text{-}C_9H_7)Ru(dppm)(H_2)]CF_3SO_3$ (**5**) to the dihydride tautomer has been observed by NMR spectroscopy. It is known that the Cp analogue of **5** does not undergo isomerization at ambient temperature too.[21]

In the $\eta^5 \rightarrow \eta^6$ haptotropic rearrangement of $[(\eta^5\text{-}C_9H_7)Ru(PPh_3)_2(H)_2]CF_3SO_3$ (**8**), the proton is likely transferred from one of the hydride ligands, as we have not detected any intermediate.

The initial products of protonation of both the dppe complex **2** and dppp complex **3** are mixtures of $\eta^2$-dihydrogen complexes and their dihydride tautomers. In both cases, the former isomerizes to the latter with increasing temperatures (Figure 1). But it can be seen from Figure 1a that at 238 K a third hydride signal, which is assignable to the $\eta^6$-indene complex $[(\eta^6\text{-}C_9H_8)Ru(dppe)H]CF_3SO_3$ (**10**), becomes visible, and this triplet increases in intensity at the expense of the

(14) (a) Stradiotto, M.; Hazendonk, P.; Bain, A. D.; Brook, M. A.; McGlinchey, M. J. *Organometallics* **2000**, *19*, 590. (b) Bonifaci, C.; Ceccon, A.; Gambaro, A.; Ganis, P.; Santi, S.; Valle, G.; Venzo, A. *Organometallics* **1993**, *12*, 4211. (c) Bonifaci, C.; Ceccon, A.; Gambaro, A.; Ganis, P.; Santi, S.; Valle, G.; Venzo, A. *J. Organomet. Chem.* **1995**, *492*, 35. (d) Kudinov, A. R.; Petrovskii, P. V.; Struchkov, Yu. T.; Yanovskii, A. I.; Rybinskaya, M. I. *J. Organomet. Chem.* **1991**, *421*, 91.

(15) (a) Jessop, P. G.; Morris, R. H. *Coord. Chem. Rev.***1992**, *121*, 155. (b) Heinekey, D. M.; Oldham, W. J., Jr. *Chem. Rev.* **1993**, *93*, 913.

(16) Chinn, M. S.; Heinekey, D. M. *J. Am. Chem. Soc.* **1990**, *112*, 5166.

(17) (a) Albright, T. A.; Hofmann, P.; Hoffmann, R.; Lillya, C. P.; Dobosh, P. A. *J. Am. Chem. Soc.* **1983**, *105*, 3396. (b) Silvestre, J.; Albright, T. A. *J. Am. Chem. Soc.* **1985**, *107*, 6829.

(18) Bianchini, C.; Meli, A.; Peruzzini, M.; Frediani, P.; Bohanna, C.; Esteruelas, M. A.; Oro, L. A. *Organometallics* **1992**, *11*, 138.

(19) Crabtree, R. H. *The Organometallic Chemistry of The Transition Metals*, 2nd ed.; John Wiley & Sons: New York, 1994; p 221.

(20) Ziegler, T.; Folga, E.; Berces, A. *J. Am. Chem. Soc.* **1993**, *115*, 636, and references therein.

(21) Conroy-Lewis, F. J.; Simpson, S. J. *J. Chem. Soc., Chem. Commun.* **1987**, 1675.

**Scheme 1**

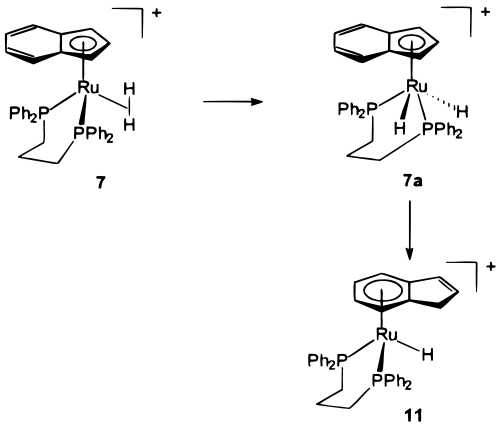


hydride signals of the dihydrogen/dihydride tautomers. At room temperature, $\eta^5 \rightarrow \eta^6$ haptotropic rearrangement is basically complete, and the only observable species in the $^1$H NMR spectrum is **10**. In this case the proton may be transferred to the indenyl ligand from the $\eta^2$-$H_2$ ligand or Ru−H or both. In the dppp system, $\eta^5 \rightarrow \eta^6$ haptotropic rearrangement, signaled by the appearance of the triplet at $\delta$ −11.37 ppm in $^1$H NMR spectroscopy, occurs at higher temperature (273 K). At this temperature, most of the dihydrogen complex has isomerized to the dihydride tautomer. Similar to the dppe system, the final thermodynamic product is the $\eta^6$-indene complex [($\eta^6$-$C_9H_8$)Ru(dppp)H]$CF_3SO_3$ (**11**).

Therefore, the variable-temperature $^1$H NMR studies indicate that $\eta^5 \rightarrow \eta^6$ haptotropic rearrangement in $\eta^5$-indenyl ruthenium dihydrogen complexes (**5**−**7**) may involve direct proton migration from the $\eta^2$-$H_2$ ligand to the indenyl ligand. Or it may involve a two-step process: proton migration from the $\eta^2$-$H_2$ ligand to the metal center to form the dihydride tautomer, followed by one of the hydride ligands undertaking an excursion to the indenyl ligand (Scheme 1).

We would like to point out that in the course of protonation of complexes **1**−**4** and subsequent $\eta^5 \rightarrow \eta^6$ haptotropic rearrangement, no free indene has ever been detected in $^1$H NMR measurements. Shapley et al. reported that protonation of ($\eta^5$-$C_9H_7$)Ir($\eta^4$-$C_8H_{12}$) ($C_8H_{12}$ = cyclooctadiene) with 1 equiv of trifluoroacetic acid at −50 °C resulted initially in the formation of free indene and a dinuclear species, [Ir($\eta^4$-$C_8H_{12}$)($\mu$-$O_2$-$CCF_3$)]$_2$, and the mixture slowly reacted to give the $\eta^6$-indene complex [($\eta^6$-$C_9H_8$)Ir($\eta^4$-$C_8H_{12}$)]$^+$. The $\eta^5$-indenylmetal hydride complex [($\eta^5$-$C_9H_7$)Ir($\eta^4$-$C_8H_{12}$)H]$^+$ was formed as an intermediate at low temperature in the presence of excess acid.[22]

Treatment of THF-$d_8$ solutions of $\eta^6$-indene complexes **9**−**12** with $Et_3N$ at room temperature quantitatively regenerated the monohydrides **1**−**4** over a period of 1 day. The reaction is presumably initiated by abstraction of an exo proton from the methylene group of the $\eta^6$-coordinated indene, generating a zwitterionic intermediate, the metal fragment of which then undergoes $\eta^6 \rightarrow \eta^5$ migration to produce the monohydride (Scheme 2). Several examples of such an arrangement, which follows deprotonation of $\eta^6$-indene complexes, have been reported.[1d−f,22] The endo protonation at the $\eta^5$-indenyl

(22) Szajek, L. P.; Shapley, J. R. *Organometallics* **1993**, *12*, 3772.

**Scheme 2**

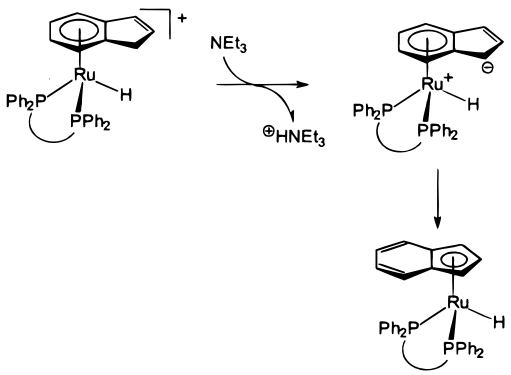


site and subsequent exo deprotonation by $Et_3N$ in our present indenyl ruthenium systems was confirmed by deuterium labeling and NMR studies. We found that deuteriation of ($\eta^5$-$C_9H_7$)Ru(dppm)D (**1-*d*$_1$**) with $CF_3SO_3D$ to generate the $\eta^6$-indene complex **9-*d*$_2$**, and its subsequent deprotonation with $Et_3N$, left a deuterium label in the five-membered ring of the resulting **1-*d*$_2$**. This is evidenced by the close to unity ratio (1.20)[23] of the integration of the $H^{1,3}$ signal to that of the $H^2$ signal (see numbering scheme in Experimental Section) in the $^1$H NMR spectrum of **1-*d*$_2$**.

Although $\eta^6$-indene complexes resulting from $\eta^5 \rightarrow \eta^6$ haptotropic rearrangement have been characterized by NMR spectroscopy, elucidation of their structures by X-ray crystallography is still rare. The molecular structure of [($\eta^6$-$C_9H_8$)Ru(dppp)H]$^+$ depicted in Figure 3 shows, unequivocally, a $\eta^6$-indene complex, in which the five-membered ring is noncoordinative.

## Conclusion

We have shown that the indenyl ruthenium complexes ($\eta^5$-$C_9H_7$)Ru($L_2$)H, upon protonation with triflic acid or $HBF_4$·$Et_2O$at −60 °C, give the dihydrogen complexes [($\eta^5$-$C_9H_7$)Ru($L_2$)($H_2$)]$^+$ or the dihydride tautomers [($\eta^5$-$C_9H_7$)Ru($L_2$)$(H)_2$]$^+$ or mixtures of both, depending on the ligands ($L_2$) used. These initial products undergo $\eta^5 \rightarrow \eta^6$ haptotropic rearrangement with increasing temperature to give the $\eta^6$-indene complexes [($\eta^6$-$C_9H_8$)Ru($L_2$)H]$^+$ as the thermodynamic products. We have reported here the first examples of such rearrangement resulting from proton migration from a $\eta^2$-$H_2$ ligand to the indenyl ligand, directly or via a dihydride intermediate, and X-ray structure of an $\eta^6$-indene ruthenium complex, which results from $\eta^5 \rightarrow \eta^6$ haptotropic rearrangement.

## Experimental Section

All manipulations were conducted under an atmosphere of nitrogen using standard Schlenk techniques. Dichloromethane was distilled from calcium hydride; tetrahydrofuran, diethyl ether, toluene, and hexane were distilled from sodium-benzophenone ketyl. THF-$d_8$ and $CD_2Cl_2$ were dried over $P_2O_5$.

(23) In theory, the ratio should be unity, the occurrence of the slightly higher ratio is due to the fact that the acid $CF_3SO_3D$ is not 100% deuterated, since it undergoes H/D exchange with residual water in the solvent.

**Table 4. Crystal Data and Refinement Details for ($\eta^5$-$C_9H_7$)Ru(dppm)H (1) and [($\eta^6$-$C_9H_8$)Ru((dppp)H]$BF_4$·$CH_2Cl_2$**

| | ($\eta^5$-$C_9H_7$)Ru(dppm)H (**1**) | [($\eta^6$-$C_9H_8$)Ru(dppp)H]$BF_4$·$CH_2Cl_2$ |
|---|---|---|
| empirical formula | $Ru(C_{34}H_{30}P_2)$ | $[RuC_{36}H_{35}P_2]BF_4$·$CH_2Cl_2$ |
| fw | 601.59 | 802.39 |
| cryst syst | triclinic | triclinic |
| space group | $P\bar{1}$ | $P\bar{1}$ |
| unit cell dimens | $a$ = 10.1792(9) Å, α = 61.013(2)° | $a$ = 10.2354(11) Å, α = 94.374(2)° |
| | $b$ = 17.836(2) Å, $\beta$ = 88.508(2)° | $b$ = 11.4412(12) Å, $\beta$ = 106.002(2)° |
| | $c$ = 18.019(2) Å, $\gamma$ = 88.208(2)° | $c$ = 16.1494(17) Å, $\gamma$ = 98.900(2)° |
| volume, $Z$ | 2860.0(4) Å$^3$, 4 | 1781.9(3) Å$^3$, 2 |
| density (calcd) | 1.397 Mg/m$^3$ | 1.495 Mg/m$^3$ |
| abs coeff | 0.681 mm$^{-1}$ | 0.727 mm$^{-1}$ |
| $F$(000) | 1232 | 816 |
| cryst size | 0.20 × 0.18 × 0.18 mm | 0.20 × 0.18 × 0.14 mm |
| wavelength | 0.71073 Å | 0.71073 Å |
| diffractometer | Bruker Smart 1000CCD | Bruker Smart 1000CCD |
| temperature | 294(2) K | 294(2) K |
| $\theta$ range for data collection | 1.29−27.55° | 1.82−27.56° |
| limiting indices | $-13 \le h \le 12$, $-23 \le k \le 23$, $-23 \le l \le 19$ | $-12 \le h \le 13$, $-14 \le k \le 12$, $-20 \le l \le 21$ |
| no. of reflns collected | 19 216 | 11 957 |
| no. of ind reflns | 12 894 ($R_{int}$ = 0.0302) | 8032 ($R_{int}$ = 0.0283) |
| abs corr | SADABS | SADABS |
| max. and min. transmn | 0.8872 and 0.8758 | 0.9051 and 0.8682 |
| refinement method | full-matrix least-squares on $F^2$ | full-matrix least-squares on $F^2$ |
| no. of data/restraints/params | 12 887/22/672 | 8032/0/442 |
| goodness-of-fit on $F^2$ | 0.851 | 0.873 |
| final $R$ indices [$I > 2\sigma(I)$] | R1 = 0.0487, wR2 = 0.1279 | R1 = 0.0491, wR1 = 0.1294 |
| $R$ indices (all data) | R1 = 0.0746, wR2 = 0.1487 | R1 = 0.0491, wR2 = 0.1429 |
| extinction coeff | 0.000(2) | 0.0000(4) |
| largest diff peak and hole | 0.904 and −0.568 e Å$^{-3}$ | 0.89 and −0.762 e Å$^{-3}$ |



The complexes ($\eta^5$-$C_9H_7$)(Ru(dppm)H (**1**),[24] ($\eta^5$-$C_9H_7$)Ru(dppe)H (**2**),[24] ($\eta^5$-$C_9H_7$)Ru(dppp)H (**3**),[24] and ($\eta^5$-$C_9H_7$)Ru($PPh_3$)$_2$H (**4**)[11a] were synthesized according to literature methods. $^1$H NMR spectra were taken on a Bruker DPX-400 spectrometer. Chemical shifts ($\delta$, ppm) were reported relative to proton residue of the deuterated solvent ($CD_2Cl_2$, $\delta$ 5.32 ppm; $CDCl_3$, $\delta$, 7.26 ppm; THF-$d_8$, $\delta$ 1.85 ppm, $\delta$ 3.70 ppm). $^{31}$P NMR spectra were taken on the Bruker DPX-400 spectrometer at 161.98 MHz. Chemical shifts were externally referenced to 85% $H_3PO_4$ in $D_2O$ ($\delta$ 0.00 ppm). $T_1$ relaxation measurements were measured at 400 MHz by inversion−recovery method using a standard 180°−$\tau$−90° pulse sequence.

**Dihydrogen Complexes [($\eta^5$-$C_9H_7$)Ru($L_2$)($H_2$)]$CF_3SO_3$ and Dihydrides [($\eta^5$-$C_9H_7$)Ru($L_2$)(H)$_2$]$CF_3SO_3$.** The dihydrogen complexes [($\eta^5$-$C_9H_7$)Ru(dppm)($H_2$)]$CF_3SO_3$ (**5**), [($\eta^5$-$C_9H_7$)Ru(dppe)($H_2$)]$CF_3SO_3$ (**6**), and [($\eta^5$-$C_9H_7$)Ru(dppp)($H_2$)]$CF_3SO_3$ (**7**) and dihydride complexes [($\eta^5$-$C_9H_7$)Ru(dppe)(H)$_2$]$CF_3SO_3$ (**6a**), [($\eta^5$-$C_9H_7$)Ru(dppp)(H)$_2$]$CF_3SO_3$ (**7a**), and [($\eta^5$-$C_9H_7$)Ru($PPh_3$)$_2$(H)$_2$]$CF_3SO_3$ (**8**) are unstable with respective to proton migration at room temperature; therefore these complexes were prepared and characterized spectroscopically in situ at low temperature.

In a typical experiment, a sample (10 mg) of the metal−hydride **1**−**4** was loaded into a 5 mm NMR tube which was then capped with a rubber septum. The tube was evacuated and filled with nitrogen gas for three cycles. Degassed THF-$d_8$ (0.4 mL) was added, via a syringe, to dissolve the sample, and the solution was then cooled to −78 °C. One equivalent of $CF_3SO_3H$ was added through a microsyringe. The tube was loaded into the NMR probe precooled to −60 °C, and the sample was immediately analyzed by NMR spectroscopy. The numbering scheme of the indenyl ligand is as follow:

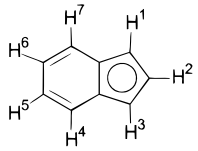


**[($\eta^5$-$C_9H_7$)Ru(dppm)($H_2$)]$CF_3SO_3$ (5).** $^1$H NMR (400 MHz, THF-$d_8$, −60 °C): $\delta$ −6.56 [br, 2H, Ru−($H_2$)], 4.15 (dt, $J$(PH) = 11.7 Hz, $J$(HH) = 15.7 Hz, 1H. PC$H$HP), 5.33 (dt, $J$(PH) = 10.8 Hz, $J$(HH) = 15.7 Hz, 1H, PCH$H$P), 5.42 (t, $J$ = 2.9 Hz, 1H, $H^2$), 5.57 (d, $J$ = 2.9 Hz, 2H, $H^{1,3}$), 7.40−7.50 (m 20 H of dppm and 4H of $H^{4-7}$). $^{31}$P{$^1$H} NMR (161.98 MHz, THF-$d_8$, −60 °C): $\delta$ 6.3 (s). $T_1$ of $\eta^2$-$H_2$ (400 MHz, THF-$d_8$), ms (temperature): 14 (218 K), 13 (223 K), 14 (233 K), 15 (243 K), 17 (253 K), 21 (263 K). A ln $T_1$ vs 1000/$T$ plot gave a $T_1$(min) of 13 ms at 228 K.

**[($\eta^5$-$C_9H_7$)Ru(dppe)($H_2$)]$CF_3SO_3$ (6).** $^1$H NMR (400 MHz, THF-$d_8$, −60 °C): $\delta$ −8.70 [br, 2H, Ru−($H_2$)], 2.53−2.97 (m, 4H, PC$H_2$C$H_2$P), 5.19 (t, $J$ = 2.9 Hz, 1H, $H^2$), 5.91 (d, $J$ = 2.9 Hz, 2H, $H^{1,3}$), 6.81 (m, 2H, $H^{4,7}$), 7.20 (m, 2H, $H^{5,6}$), 7.40−7.70 (m, 20H of dppe). $^{31}$P{$^1$H} NMR (161.98 MHz, THF-$d_8$, −60 °C): $\delta$ 85.4 (s). $T_1$ of $\eta^2$-$H_2$ (400 MHz, THF-$d_8$), ms (temperature): 25 (208 K), 16 (223 K), 15 (233 K), 18 (243 K), 25 (253 K), 32 (273 K). A ln $T_1$ vs 1000/$T$ plot gave a $T_1$(min) of 17 ms at 231 K.

**[($\eta^5$-$C_9H_7$)Ru(dppp)($H_2$)]$CF_3SO_3$ (7).** $^1$H NMR (400 MHz, THF-$d_8$, −60 °C): $\delta$ −7.96 [br, 2H, Ru−($H_2$)], 1.39−2.70 (m, 6H, PC$H_2$C$H_2$C$H_2$P), 5.42 (t, $J$ = 2.9 Hz, 1H, $H^2$), 5.83 (d, $J$ = 2.9 Hz, 2H, $H^{1,3}$), 7.30−7.70 (m, 20H of dppp and 4H of $H^{4-7}$). $^{31}$P{$^1$H} NMR (161.98 MHz, THF-$d_8$, −60 °C): $\delta$ 55.4 (s). $T_1$ of $\eta^2$-$H_2$ (400 MHz, THF-$d_8$), ms (temperature): 18 (218 K), 16 (223 K), 15 (228 K), 16 (233 K), 23 (253 K). A ln $T_1$ vs 1000/$T$ plot gave a $T_1$(min) of 15 ms at 231 K.

**[($\eta^5$-$C_9H_7$)Ru(dppe)H$_2$]$CF_3SO_3$ (6a).** $^1$H NMR (400 MHz, THF-$d_8$, −60 °C): $\delta$ −8.70 (t, $J$(HP) = 29.3 Hz, 2H, Ru-$H_2$), 2.46−2.90 (m, 4H, PC$H_2$C$H_2$P), 5.12 (t, $J$ = 2.9 Hz, 1H, $H^2$),

(24) (a) Gamasa, M. P.; Gimeno, J.; Gonzalez-Bernardo, C.; Martín-Vaca, B. M.; Monti, D.; Bassetti, M. *Organometallics* **1996**, *15*, 302. (b) Bassetti, M.; Casellato, P.; Gamasa, M. P.; Gimeno, J.; González-Bernardo, C.; Martin, Vaca, B. *Organometallics* **1997**, *16*, 5470.

5.92 (d, $J$ = 2.9 Hz, 2H, $H^{1,3}$), 6.81 (m, 2H, $H^{4,7}$), 7.20 (m, 2H, $H^{5,6}$), 7.40−7.70 (m, 20H of dppe). $^{31}P\{^1H\}$ NMR (161.98 MHz, THF-$d_8$, −60 °C): $\delta$ 75.7 (s). $T_1$ of Ru−H (400 MHz, THF-$d_8$), ms (temperature): 356 (208 K), 207 (223 K), 325 (233 K), 268 (243 K), 401 (253 K). A ln $T_1$ vs 1000/$T$ plot gave a $T_1$(min) of 203 ms at 226 K.

**[($\eta^5$-$C_9H_7$)Ru(dppp)$H_2$]$CF_3SO_3$ (7a).** $^1$H NMR (400 MHz, THF-$d_8$, −60 °C): $\delta$ −98.85 (t, $J$(HP) = 29.3 Hz, 2H, Ru$H_2$), 1.40−3.10 (m, 6H, PC$H_2$C$H_2$C$H_2$P), 4.49, (t, $J$ = 2.9 Hz, 1H, $H^2$), 5.64 (d, $J$ = 2.9 Hz, 2H, $H^{1,3}$), 7.10−7.70 (m, 20H of dppp and 4H of $H^{4-7}$). $^{31}P\{^1H\}$ NMR (161.98 MHz, THF-$d_8$, −60 °C): $\delta$ 43.5 (s). $T_1$ of Ru−H (400 MHz, THF-$d_8$), ms (temperature): 499 (218 K), 412 (223 K), 364 (228 K), 426 (233 K), 373 (238 K), 850 (253). A ln $T_1$ vs 1000/$T$ plot gave a $T_1$(min) of 354 ms at 231 K.

**[($\eta^5$-$C_9H_7$)Ru($PPh_3$)$_2H_2$]$CF_3SO_3$ (8).** $^1$H NMR (400 MHz, THF-$d_8$, −60 °C): $\delta$ −9.25 (t, $J$(HP) = 24.8 Hz, 2H Ru$H_2$), 5.62 (d, $J$ = 2.9 Hz, 2H, $H^{1,3}$), 5.70 (t, $J$ = 2.9 Hz, 1H, $H^2$), 5.96−6.90 (m, 4H, $H^{4-7}$), 7.30 (m, 30H of $PPh_3$). $^{31}P\{^1H\}$ NMR (161.98 MHz, THF-$d_8$, −60 °C): $\delta$ 61.0 (s). $T_1$ of Ru−H (400 MHz, THF-$d_8$), ms (temperature): 1494 (203 K), 857 (213 K), 815 (218 K), 664 (223 K), 531 (233 K), 451 (243 K), 398 (253 K) 309 (273 K).

The corresponding HD isotopomers of **5**−**7** were prepared analogously except that $CF_3SO_3D$ was used in place of $CF_3SO_3H$. The $\eta^2$-HD signals were observed after nulling the $\eta$-$H_2$ peaks by the inversion−recovery method.

**[($\eta^5$-$C_9H_7$)Ru(dppm)(HD)]$CF_3SO_3$ (5-$d_1$).** $^1$H NMR (400 MHz, −60 °C): $\delta$ −6.60 [t, $^1J$(HD) = 25.9 Hz, 1H, Ru($H$D)].

**[($\eta^5$-$C_9H_7$)Ru(dppe)(HD)]$CF_3SO_3$ (6-$d_1$).** $^1$H NMR (400 MHz, THF-$d_8$, −60 °C): −8.72 [t, $^1J$(HD) = 29.4 Hz, 1H, Ru($H$D)].

**[($\eta^5$-$C_9H_7$)Ru(dppp)(HD)]$CF_3SO_3$ (7-$d_1$).** $^1$H NMR (400 MHz, THF-$d_8$, −60 °C): $\delta$ −7.99 [t, $^1J$(HD) = 27.4 Hz, 1H, Ru(HD)].

The $\eta^6$-indene complexes **9**−**12** were prepared in situ by warming the THF-$d_8$ solutions of **5**, **6** and **6a**, **7** and **7a**, and **8**, respectively, to room temperature. The complexes were characterized by NMR spectroscopy. Chemical shifts of Ru−H and the $\eta^6$-indene protons are summarized in Table 1.

**[($\eta^6$-$C_9H_8$)Ru(dppm)H]$CF_3SO_3$ (9).** $^1$H NMR (400 MHz, THF-$d_8$, 20 °C): $\delta$ 4.26 (dt. $J$(HH) = 15.7 Hz, $J$(HP) = 11.7 Hz, 1H, PC$H$HP), 5.46 (dtd, $J$(HP) = 10.8 Hz, $J$(HH) = 3.9 Hz, $J$(HH) = 15.7 Hz, 1H, PCH$H$P), 7.40−7.60 (m, 20H of dppm). $^{31}P\{^1H\}$ NMR (161.98 MHz, THF-$d_8$, 20 °C): $\delta$ 11.8 (s).

**[($\eta^6$-$C_9H_8$)Ru(dppe)H]$CF_3SO_3$ (10).** $^1$H NMR (400 MHz, THF-$d_8$, 20 °C): $\delta$ 2.00−3.00 (m, 4H, PC$H_2$C$H_2$P), 7.50−7.60 (m, 20H of dppe). $^{31}P\{^1H\}$ NMR (161.98 MHz, THF-$d_8$, 20 °C): $\delta$ 88.6 (s).

**[($\eta^6$-$C_9H_8$)Ru(dppp)H]$CF_3SO_3$ (11).** $^1$H NMR (400 MHz, THF-$d_8$, 20 °C): $\delta$ 2.10−3.00 (m, 6H, PC$H_2$C$H_2$C$H_2$P), 7.40−7.55 (m, 20H of dppp). $^{31}P\{^1H\}$ NMR (161.98 MHz, THF-$d_8$, 20 °C): $\delta$ 40.2 (s).

**[($\eta^6$-$C_9H_8$)Ru($PPh_3$)$_2$H]$CF_3SO_3$ (12).** $^1$H NMR (400 MHz, THF-$d_8$, 20 °C): $\delta$ 6.80−7.30 (m, 30H of $PPh_3$). $^{31}P\{^1H\}$ NMR (161.98 MHz, THF-$d_8$, 20 °C): $\delta$ 57.2 (s).

**Crystallographic Studies.** Yellow crystals of **1** and orange crystals of [($\eta^6$-$C_9H_8$)Ru(dppp)H]$BF_4$·$CH_2Cl_2$ suitable for X-ray diffraction studies were obtained as described in the Results section. Relevant data-collection and structure-refinement information is summarized in Table 4.

**Acknowledgment.** The authors acknowledge the financial support from the Hong Kong Research Grant Council (Earmarked Grant PolyU 5153/98P).

**Supporting Information Available:** Tables of atomic coordinates and equivalent isotropic displacement coefficients, complete bond lengths and angles, anisotropic displacement coefficients, and isotropic displacement coefficients for ($\eta^5$-$C_9H_7$)Ru(dppm)H and [($\eta^6$-$C_9H_8$)Ru(dppp)H]$BF_4$·$CH_2Cl_2$.This material is available free of charge via the Internet at http://pubs.acs.org.

OM000266E